A Mechanism for Precision-Sensing via a Gradient-Sensing Pathway: A Model of *Escherichia coli* Thermotaxis

Lili Jiang,[†‡] Qi Ouyang,[†] and Yuhai Tu[‡*]
[†]Center for Theoretical Biology and School of Physics, Peking University, Beijing 100871, China; and [‡]IBM T. J. Watson Research Center, Yorktown Heights, New York 10598

ABSTRACT Thermotaxis is the phenomenon where an organism directs its movement toward its preferred temperature. So far, the molecular origin for this precision-sensing behavior remains a puzzle. We propose a model of *Escherichia coli* thermotaxis and show that the precision-sensing behavior in *E. coli* thermotaxis can be carried out by the gradient-sensing chemotaxis pathway under two general conditions. First, the thermosensor response to temperature is inverted by its internal adaptation state. For *E. coli*, chemoreceptor Tar changes from a warm sensor to a cold sensor on increase of its methylation level. Second, temperature directly affects the adaptation kinetics. The adapted activity in *E. coli* increases with temperature in contrast to the perfect adaptation to chemical stimuli. Given these two conditions, *E. coli* thermotaxis is achieved by the cryophilic and thermophilic responses for temperature above and below a critical temperature T_c, which is encoded by internal pathway parameters. Our model results are supported by both experiments with adaptation-disabled mutants and the recent temperature impulse response measurements for wild-type cells. T_c is predicted to decrease with the background attractant concentration. This mechanism for precision sensing in an adaptive gradient-sensing system may apply to other organisms, such as *Dictyostelium discoideum* and *Caenorhabditis elegans*.

INTRODUCTION

One of the main challenges in modern biology is to understand the molecular mechanisms for the cellular decision-making processes in response to complex chemical and physical environmental changes. Temperature is one of the most ubiquitous environmental factors that affect the behaviors of living organisms. Bacteria and other higher organisms can sense changes in temperature and move to a preferred temperature, i.e., thermotaxis. Though much progress has been made in characterizing the thermotaxis behaviors in organisms from *Escherichia coli* to *Caenorhabditis elegans*, their molecular mechanisms remain largely unknown, partly because of the ubiquity of the temperature effects. For *E. coli* thermotaxis, it was established by Maeda and Imae (1) and Mizuno and Imae (2) that the thermotactic behavior is governed by the same signaling pathway responsible for *E. coli* chemotaxis, one of the best-studied signaling systems in biology (3–5). Thus, *E. coli* thermotaxis provides us a rare opportunity to study the mechanism for this important temperature-dependent behavior at the molecular level. For *E. coli*, the methyl-accepting chemotaxis protein (MCP) chemoreceptors also serve as the thermosensor. Analogous to ligand binding in chemotaxis, temperature affects the chemoreceptor conformational changes and affects the autophosphorylation rate of the histidine kinase CheA (attached to the MCP through the adaptor protein CheW). CheA-P then transfers its phosphate group to the response regulator CheY. CheY-P diffuses within the cytoplasm and binds to the flagellar motor complex, reversing the rotation of flagella from counterclockwise to clockwise, which causes the cell to tumble. The adaptation to persistent stimuli is accomplished by two enzymes: the methylesterase CheB, which on activation through phosphorylation by CheA-P can remove methyl groups from chemoreceptors and decrease their kinase activities; and methyltransferase CheR, which adds methyl groups to chemoreceptors and increases their activities.

Despite their commonality, there are significant differences between *E. coli* thermotaxis and chemotaxis. Unlike chemotaxis, in which increasing attractant concentration always decreases the receptor kinase activity, the response to higher temperature could either suppress (warm sensing) or enhance (cold sensing) the receptor kinase activity, depending on the receptor methylation level. It was shown in a series of pioneering experiments by Mizuno and Imae (2) and Nishiyama et al. (6) that one of the major chemoreceptors, Tar, switches from warm sensing to cold sensing as the receptor methylation level m increases pass a critical level $m_c = 2$ (QEQE). Behavior-wise, instead of always going up (down) an attractant (repellent) gradient, i.e., gradient sensing in chemotaxis, the cells seem to migrate to a particular temperature (7), which requires precision sensing. Recently, several quantitative measurements on thermotaxis have been carried out by using laser heating to study the response of *E. coli* to controlled spatial (8) and temporal (9) temperature profiles. It was found in Paster and Ryu (9) that the response to a temperature impulse is inversed as the base temperature increases pass certain critical value, in contrast to the response to ligand impulse, where the response is independent of the background ligand concentration. In Salman and Libchaber (8), it was discovered that *E. coli* thermotaxis behavior depends strongly on

Submitted February 20, 2009, and accepted for publication April 21, 2009.

*Correspondence: yuhai@us.ibm.com

Editor: Jason M. Haugh.

0006-3495/09/07/0074/9 $2.00

doi: 10.1016/j.bpj.2009.04.029

the chemical background and the growth condition of the cells. Taken together, these experimental works raise a set of important questions on thermotaxis. How could a signaling pathway designed for gradient sensing (chemotaxis) also lead the cell toward a particular temperature (thermotaxis)? Where is the preferred temperature encoded in the internal signaling pathway? How does the preferred temperature depend on the external environment? So far, very little theoretical/modeling work has been proposed to address these questions.

In this study, we develop a general mathematical description of *E. coli* thermotaxis by extending a model for chemotaxis to include temperature effects. We identify two temperature effects that are crucial for precision sensing in thermotaxis. First, we find that temperature can strongly affect the way receptor methylation level modulates the receptor kinase activity. Earlier thermotaxis experiments by Mizuno and Imae (2) for cheRcheB mutant can be explained by including a temperature dependent methylation energy in the total free energy governing the receptor kinase activity. Second, we find that temperature can strongly affect the adaptation kinetics. Temperature not only changes the adaptation time, more importantly it directly changes the adapted kinase activity, effectively rendering the temperature adaptation imperfect, in contrast to adaptation to chemical signal, such as aspartate. We show that both of these temperature dependences are needed in understanding the inverted response to temperature changes as the base temperature increases over a critical temperature. Whereas the energetic effects of temperature (condition 1), specifically the temperature dependence of the methylation free energy, makes the inverted response possible; it is the temperature dependent imperfect adaptation kinetics, i.e., condition 2, that drives the receptors to the higher receptor methylation levels where the inverted response occurs. The dependence of the critical temperature on internal pathway parameters is obtained from our model. We find that the preferred temperature is encoded predominantly in the adaptation part of the pathway. In addition to explaining the inverted responses as seen in the recent impulse response experiments, the observed overshoot in the response for base temperature below the critical temperature also comes out naturally from our model. Our model can also be used to study integration and interference between chemical and thermal stimuli. The critical (inversion) temperature is predicted to decrease with the background attractant ligand concentration. Finally, we suggest that the general mechanism for precision sensing may provide insights in studying other precision-sensing systems, such as thermotaxis in *C. elegans* and *Dictyostelium*.

A model for *E. coli* thermotaxis

We develop a *E. coli* thermotaxis model by including key temperature effects in a general chemotaxis model recently developed by Tu et al. (10). Briefly, the *E. coli* thermotaxis signaling pathway is composed of two key parts with two different timescales. Changes of the chemoreceptor activity are fast and can be described by using a quasi-equilibrium approximation. The adaptation kinetics is slower and can be described by an ordinary differential equation governing the receptor methylation level dynamics. Temperature can affect all the biochemical processes including ligand binding, methylation kinetics and kinase activity as illustrated in Fig. 1. The kinase activity of a functional cluster containing N receptor dimers is given by:

$$a(m,[L],T) = (1 + \exp(f_t(m,[L],T,N)))^{-1}, \quad (1)$$

where f_t is the total free energy difference between the active and inactive state of the functional cluster, which can be written as:

$$f_t(m,[L],T,N) = N[f_m(m,T) + f_L([L],T)], \quad (2)$$

where m is the average methylation level of the chemoreceptors, T stands for temperature, and $[L]$ represents ligand concentration. $f_m(m,T)$ and $f_L([L],T)$ are the methylation and ligand concentration dependent free energies, both dependent on temperature. All free energies here are expressed in units of the thermal energy K_BT, with K_B the Boltzmann constant. For the methylation free energy, we can approximate its temperature dependence by linear expansion around a reference temperature T_0:

$$f_m(m,T) \approx f_m(m,T_0) + \alpha(m)(T-T_0) \approx E_m(m_0-m) + \alpha(m)(T-T_0). \quad (3)$$

Following Tu et al. (10), we approximate $f_m(m,T_0)$ in the above equation by a linear function of m with two positive parameters E_m, m_0 (<2), both of which could depend on the

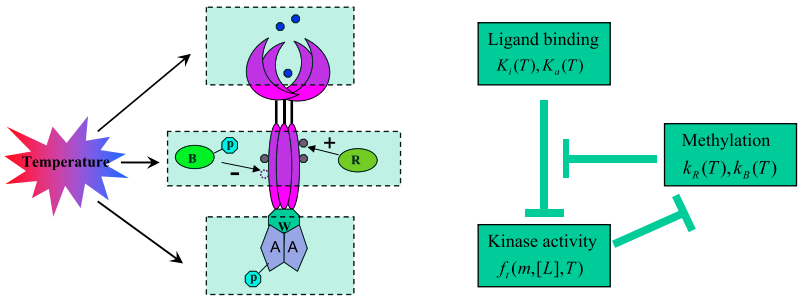

FIGURE 1 Illustration of the key temperature effects in chemotaxis pathway. Three major components of the chemotaxis pathway (receptor ligand binding, methylation and demethylation of the chemoreceptors by CheR and CheB-P, respectively, and CheA kinase activity) are shown. A corresponding block diagram of the pathway model is shown on the right. The kinase activity is decreased by attractant ligand binding. The suppression of kinase activity is balanced by a slow increase in ligand methylation level. This adaptation process is in turn controlled by the kinase activity.

reference temperature T_0. The function $\alpha(m)$ characterizes the response to temperature for a given receptor methylation level m. It can be different for different species of chemoreceptors, such as Tar and Tsr. The ligand concentration dependent part of the free energy $f_L([L],T)$ can be described by the MWC type model (11–13):

$$f_L([L],T) = \ln((1 + [L]/K_i(T))/(1 + [L]/K_a(T))), \quad (4)$$

K_i and $K_a(= K_i/C)$ are the dissociation constants of the inactive and active receptors respectively, both of them can depend on temperature.

Given the large number of possible combinatory methylation states for the chemoreceptor complex, the average methylation level m can be approximated as a continuum variable. The dynamics for the methylation level m is dictated by the perfect adaptation to ligand concentration (14–16) and can be written generally by following Tu et al. (10):

$$\begin{aligned} dm(t)/dt &= F(a,T) \approx k_R(1-a) - k_B a \\ &\equiv (a_0(T) - a)/\tau_m(T). \end{aligned} \quad (5)$$

For simplicity, we have approximated the methylation rate function $F(a,T)$ by a linear form in a in the above equation, with the steady-state activity and the linear methylation timescale represented by a_0 and τ_m, respectively. This linear approximation is equivalent to allowing only inactive receptors to be methylated and only active receptors to be demethylated with the corresponding linear rates $k_R(T)$ and $k_B(T)$. These two chemical reaction rates are both temperature dependent, and their ratio can be written as $k_R/k_B = \exp[\Delta G_{RB}(T)/(K_B T)]$, where $\Delta G_{RB}(T)$ is the difference between the two activation energies for the methylation and demethylation reactions. Let T_0 be the temperature at which $\Delta G_{RB}(T_0) = 0$ and, given the relative small range of temperature considered, we can approximate $\Delta G_{RB}(T)/(K_B T)$ by linear expansion around T_0: $\Delta G_{RB}(T)/(K_B T) \approx \beta(T - T_0)$ with a constant β. Therefore, the adapted activity at steady state can be approximated as:

$$a_0(T) = k_R/(k_R + k_B) \approx 1/(1 + \exp(-\beta(T - T_0))). \quad (6)$$

The methylation timescale τ_m can also depend on temperature. We assume it approximately decays exponentially with temperature: $\tau_m(T) \equiv (k_R + k_B)^{-1} \approx \tau_0 e^{-T/T_m}$, with constant τ_0 and T_m. More complex forms of $F(a,T)$, such as those based on Michaelis-Menten kinetics of CheR and CheB-P (17), can be used, but they do not change the conclusions of this study.

From Eq. 6, we see that the adaptation to constant chemical stimuli is perfect, i. e., the steady-state kinase activity $a_0(T)$ is independent of the ambient ligand concentration as $[L]$ does not affect adaptation kinetics directly. However, $a_0(T)$ does vary with the background temperature. This imperfect adaptation to temperature comes naturally because temperature directly affects the adaptation kinetics, and the temperature dependences of the methylation and demethylation rates are not the same, i.e., $\beta \neq 0$. Indeed, the increase of $a_0(T)$ with temperature T is consistent with recent fluorescence resonance energy transfer (FRET) measurements of the adapted kinase activities at different temperatures (T. Shimizu, unpublished).

By including temperature effects in a general chemotaxis model, we now have a model for thermotaxis signaling. The details of this thermotaxis model are specified by a few key parameters $\alpha(m)$, β, and $K_{i,a}(T)$ that describe the temperature effects in methylation free energy, adaptation kinetics and ligand binding respectively. It is difficult to calculate these quantities from first principles. Our model allows us to estimate their forms and values by connecting them with various existing (and future) experiments. At present, not enough experimental data are available to uniquely determine all the parameters. To carry out quantitative simulations of our model in this study, we use a reasonable set of parameters $m_0 = 1.9$, $E_m = 1$, and $\beta = 0.12°C$ at the reference temperature $T_0 = 32°C$, chosen by the requirement $a_0(T_0) = 0.5$ and guided by recent FRET experiments, which show a_0 (22°C) $\approx$ 0.3 and a_0 (32°C) $\approx$ 0.5 (T. Shimizu, unpublished); the pathway parameters $N = 6$ and $C = 0.01$ are taken from Mello and Tu (13) and $K_i(T_0) = 36$ μM is used at T_0; methylation timescale and its temperature dependence are set by $\tau_0 = 120$ s and $T_m = 10°C$. Other choices of parameters have been used without altering the conclusions of this study. Our main focus in this study is to understand the general mechanism for precision sensing independent of the quantitative details. Specifically, by studying the model for *E. coli* thermotaxis, we aim to uncover the general conditions that make the system capable of detecting a particular temperature by using a pathway known primarily for sensing gradients of external signals.

RESULTS

Temperature response depends on receptor methylation level: the inverted thermoresponse for chemoreceptor Tar in the cheRcheB mutants

The thermosensing ability of *E. coli* was studied extensively by Imae et al. (7) by using temperature profile controlled by water flow. They used various cheRcheB mutants in which the adaptation process is disabled and the MCP receptors are fixed in different states of modification. They showed that the thermosensing function of the aspartate chemoreceptor Tar is modulated by covalent modification of its four methylation sites (18). It was found that without post-translational deamidation Tar has no thermosensing ability, whereas the unmethylated and highly methylated receptors function as warm and cold sensors, respectively. This observed methylation-dependent response to temperature can be described by the coupling term between temperature and the methylation level in our model. Specifically, the $\alpha(m)(T - T_0)$ term in the methylation free energy and the

form of $\alpha(m)$ determine the kinase response to temperature change for a given receptor methylation level. For Tar, we set $\alpha(m) = \alpha_0(m_c - m)$ with $\alpha_0 \geq 0$ as guided by experiments (18) with the crossover methylation level m_c being that of the unmodified native receptor with $m_c = 2$. We choose $\alpha_0 = 0.3^\circ$C in this study. The thermoresponses calculated from our model are shown in Fig. 2 for the warm sensor with $m = 1.8$ (<2) and the cold sensor with $m = 2.15$ (>2) to temperature profile similar to that used in the original experiments. As expected, our mathematical model reproduces the inverted response at high methylation levels ($m > 2$), in agreement with previous experiments (18).

Thermotaxis in wt *E. coli* cells: imperfect adaptation to temperature drives the inverted thermoresponse

Adaptation is an essential component for biological sensory system. For *E. coli*, adaptation to chemical stimulus is highly accurate (19) and this property of perfect adaptation is robust against changes in protein concentrations (14,20). The conditions for and the consequences of this (near) perfect adaptation are studied over the past 10 years (14–16). It is now understood how such (near) perfect adaptation can maintain high sensitivity for gradient sensing in a wide range of background ligand concentrations (13). However, thermotaxis operates in a relatively narrow range of temperature. It also differs from gradient sensing in chemotaxis as it is aimed at sensing/determining a particular (preferred) temperature. In this section, we show that the adapted activity depends on temperature and such imperfect adaptation (to temperature) is essential for precision sensing and the inverted response to temperature increase as observed in the recent thermo-impulse experiments by Paster and Ryu (9).

For a given temperature T, the steady-state Tar methylation level $m_s(T)$ can be determined by setting $dm/dt = 0$ in Eq. 5:

$$m_s(T) = ((N\alpha_0 m_c + \beta)(T - T_0) + NE_m m_0)/(N(\alpha_0(T - T_0) + E_m)). \quad (7)$$

As shown by Nishiyama et al. (18) experimentally and described mathematically in our model in the last section, receptor Tar switches its response from warm sensing to cold sensing as its methylation level rises beyond a certain threshold value $m_c (= 2)$. Therefore, the transition temperature T_c for warm sensor to cold sensor can be determined by $m_s(T_c) = m_c$, which leads to the expression for the critical temperature T_c:

$$T_c = T_0 + NE_m(m_c - m_0)/\beta. \quad (8)$$

For $T \leq T_c$, the cells are warm sensing because steady-state receptor methylation is $m_s \leq m_c$; therefore, the response to a temperature increase will be a decrease in receptor kinase activity. For $T > T_c$, we have $m_s > m_c$; therefore, the response to a further increase in temperature is an increase in the receptor kinase activity, similar to the response to a chemical repellent. This reversal of response allows the cell to migrate to the preferred temperature T_c. Quantitatively, from Eq. 8 and the parameters used in this study,

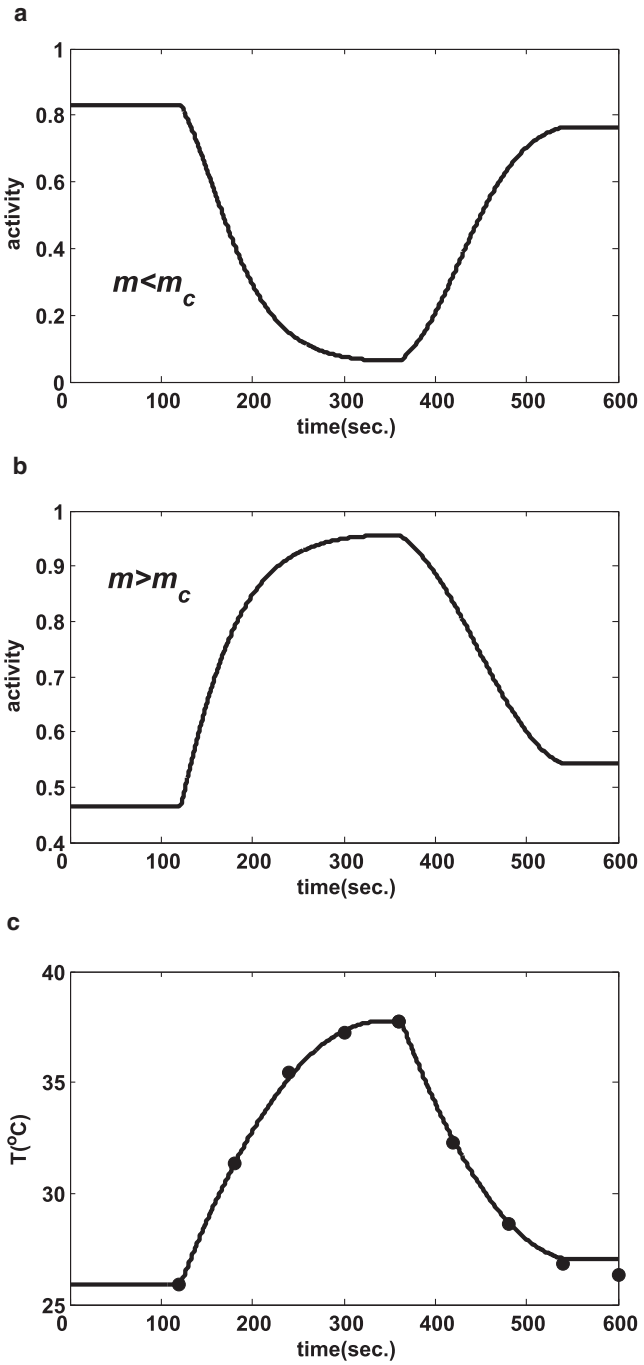

FIGURE 2 Inverted thermoresponse for different cheRcheB mutants with different receptor methylation levels. Responses to the same temperature profile are shown for receptors with different average methylation levels: (*a*) $m = 1.8 < m_c$ and (*b*) $m = 2.15 > m_c$, which function as warm and cold sensors, respectively. The temperature profile shown in *c* has the same shape of time dependence as the experimental data (*solid circles*) published in Nishiyama et al. (18).

$T_c \approx 37°C$ is consistent with existing experimental observations (7,9).

Equations 7 and 8 show the conditions for the existence of the inverted response and how the critical temperature is encoded in the pathway. The reversed response as methylation level increases, i.e., the existence of the critical methylation level m_c, is necessary but not sufficient for the reversed response to temperature in wt cell. The adaptation kinetics, in particular the imperfect adaptation to temperature, is needed to drive the system to methylation level higher than m_c. This is achieved in our model by having a nonzero positive β. If the adaptation to temperature were perfect with $\beta = 0$ from Eq. 7 the steady-state methylation would always stay either below or above m_c for $m_0 < m_c$ or $m_0 > m_c$, respectively. Correspondingly the wt cell would be either warm sensing or cold sensing for all temperatures ($T_c \rightarrow \infty$ from Eq. 8), thus incapable of precision sensing. According to this mechanism for the inverted response, the critical temperature is encoded mainly in the methylation part of the pathway. In particular, T_c depends on how temperature affects the methylation free energy (e.g., the existence and the value of m_c) and how the methylation kinetics depends on temperature (e.g., β). In our model with $\alpha_0 > 0$, the critical temperature T_c can be either attractive or repulsive depending on the sign of β. For $\beta > 0$, i.e., when the adapted activity increases with temperature as we have assumed in this study, the cells are attracted to the critical temperature T_c. For $\beta < 0$, i.e., if the adapted activity decreases with T, T_c becomes repulsive: cells will move away from it. This repulsive thermotaxis behavior seems to be present in *Dictyostelium discoideum* (21). Taken together, precision sensing is possible and a critical temperature T_c exists only when both conditions $\alpha_0 \neq 0$ and $\beta \neq 0$ are satisfied. T_c is attractive for $\alpha_0\beta > 0$ and repulsive for $\alpha_0\beta < 0$. A detailed derivation of these precision-sensing conditions, independent of the simplifying linear approximations used in this study is provided in the Supporting Material.

The presence and absence of overshoot in temperature impulse response for base temperature below and above T_c, respectively

We have also studied the response of the wt cells to an impulse signal $T = T_b + \Delta T \exp(-(t - t_0)/\tau)$ for $t \geq t_0$, the same as used in the recent experiments by Paster and Ryu (9). T_b is the base temperature for $t < t_0$, $\Delta T > 0$ is the temperature jump at $t = t_0 = 10$ s and $\tau = 12.5$ s is the recovery time ($T(t)$ is shown in Fig. 3 *c*). The impulse responses from our model for base temperature below and above the critical temperature T_c are shown in Fig. 3, *a* and *b*, *thick lines*. In agreement with the experimental observation made in Paster and Ryu (9), we find that the response to temperature impulse with $T_b \leq T_c$ has an overshoot similar to the impulse response in chemotaxis; but the overshoot is absent for $T_b > T_c$. Similar difference in responses to step function change in temperature for $T_b \leq T_c$ and $T_b > T_c$ is shown in Supporting Material and Fig. S1. The simulations in this study are done with only Tar receptor, and we do not expect any qualitative difference in temperature impulse response by also including Tsr receptor in our model. The general effects of Tsr in thermotaxis are discussed later in the Discussion section.

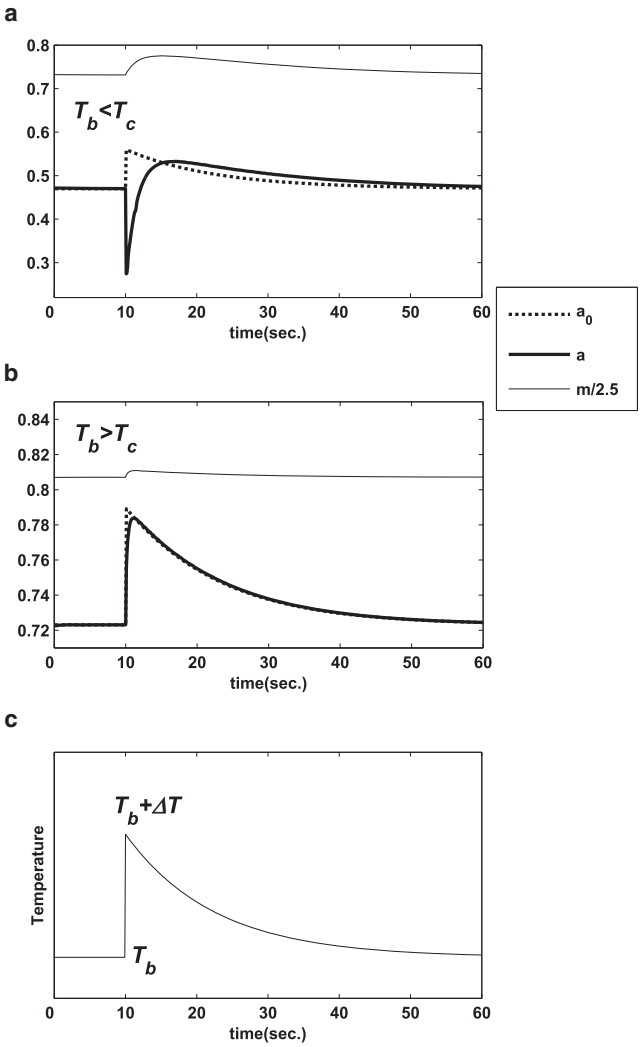

FIGURE 3 The inverted response to a temperature impulse in wild-type cells as the base temperature increases pass a critical temperature T_c. (*a*) The positive response to temperature impulse at $T_b = 31°C < T_c$. Activity $a(t)$ (*thick line*) decreases right after the onset of the temperature impulse and eventually recovers to its prestimulus level with an overshoot. The steady-state activity $a_0(T(t))$ and the receptor methylation level are plotted by dotted line and thin solid lines, respectively. After the time when the methylation level reaches its maximum value, the instantaneous activity (*thick line*) moves above the steady-state activity (*dotted line*) as shown from our model. This explains the experimentally observed overshoot (9). (*b*) Negative response to temperature impulse at $T_b = 40°C > T_c$. The initial response to the temperature impulse is an increase in activity. Therefore, there is no overshoot in the dynamics of the activity. The temperature impulse profile is shown in *c*, where temperature rapidly increases from T_b to $T_b + \Delta T$ at the onset ($\Delta T = 3°C$ as in the experiments (9)) and then decays exponentially back to T_b with a time constant $\tau = 12.5$ s.

We now explain the presence or absence of the overshoot for temperature impulse by analyzing the methylation kinetics given by Eq. 5: $dm/dt = (a_0(T(t)) - a)/\tau_m$. The adapted steady-state kinase activity $a_0(T(t))$, shown as the dotted line in Fig. 3, *a* and *b*, is determined by the instantaneous temperature and follows the same trend as $T(t)$ shown in Fig. 3 *c*. For impulse signal with low base temperature $T_b < T_c$, the activity rapidly decreases below the baseline activity $a_0(T_b)$ at the onset of the impulse. This initial decrease in activity leads to the first (downward) lobe of the activity response curve (Fig. 3 *a*), in which methylation level (Fig. 3, *a* and *b*, *thin sold line*) increases quickly according to Eq. 5. However, eventually the methylation level recovers to its initial value as the temperature return to its preimpulse level. Therefore, there exists a time $t_c(>t0)$, beyond which methylation level start to decrease $dm/dt|_{t>t_c} < 0$. From Eq. 5, we then have $a(t) > a_0(T(t)) > a_0(T_b)$ for $t > t_c$. Putting it together with the fact that the kinase activity $a(t)$ drops below $a_0(T_b)$ right after the start of the impulse, the existence of the impulse response overshoot for $T_b < T_c$ becomes evident. On the other hand, for $T_b > T_c$, the immediate response to the temperature impulse is the increase of the kinase activity above $a_0(T_b)$. Therefore, in the inverted response regime, the kinase activity stays above $a_0(T_b)$ for the whole duration of the pulse stimulus and there is no overshoot in kinase response. This direct connection between the inverted response and the overshoot to temperature impulse as shown by our model thus explains the recent impulse response measurements by Paster and Ryu (9), and the agreement with the experiments further verifies our model.

Chemical and thermal signal interference and integration: chemical backgrounds affect thermotaxis

As shown in the previous section, imperfect adaptation can induce an inverse of *E. coli* thermo-impulse response at a particular temperature in the absence of any ligand. We discuss the effects of chemical background on the inverse temperature T_c. In steady state, the receptor methylation level can be determined by Eqs. 1–6:

$$m_s(T,[L]) = (N(E_m m_0 + 2\alpha_0(T - T_0) + \ln((1 + [L]/K_i(T))/(1 + [L]/K_a(T)))) + \beta(T - T_0))/(N(E_m + \alpha_0(T - T_0))), \quad (9)$$

where $[L]$ is the background attractant ligand concentration. The instantaneous thermo-impulse response of *E. coli* is determined by adapted methylation level at the background temperature. *E. coli* responses positively to temperature increase (warm sensing) when $m < m_c$ and negatively (cold sensing) when $m > m_c$. Therefore, the inverse temperature can be determined by setting steady-state $m_s(T,[L]) = m_c$. From Eq. 9, we obtain the critical temperature and its dependence on the ligand concentration for the case where $K_{i(a)}$ are independent of T:

$$T_c([L]) = T_c(0) - N[\ln(1 + [L]/K_i) - \ln(1 + [L]/K_a)]/\beta, \quad (10)$$

where $T_c(0)$ is the inversion temperature in the absence of ligand, given by Eq. 8. Equation 10 shows that the critical temperature decreases with increasing attractant ligand concentration, as verified by direct simulation of our model shown in Fig. 4. The decrease in T_c is caused by the receptor methylation level increases with background attractant concentration. This reduction in the critical temperature in the presence of attractant is one of the predictions of our model, which can be tested experimentally.

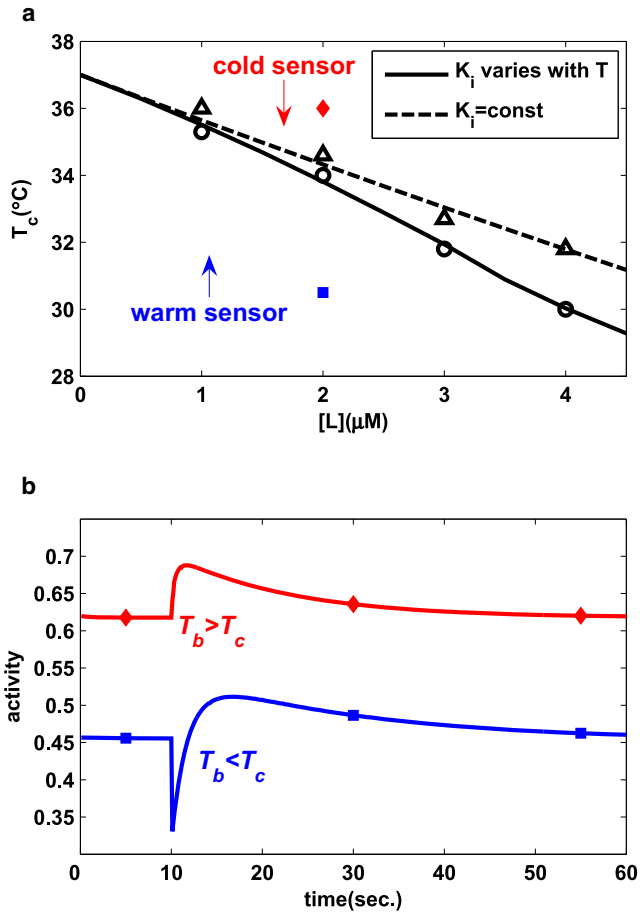

FIGURE 4 The dependence of the critical temperature on the background attractant concentration. (*a*) The critical temperature at different background attractant concentrations. Higher concentration of background attractant level decreases the inversion temperature. If K_i increases with temperature, e.g., $K_i = K_i(T_0)\exp[(T - T_0)/T_K]$ with $T_K = 10°C$, the critical temperature (*solid line*) T_c decreases further as compared with the case with constant K_i (*dotted line*). (*b*) The positive and negative responses to a temperature impulse (the same as described in Fig. 3 *c*). Two response curves with $T_b < T_c$ (*lower curve with squares*) and $T_b > T_c$ (*upper curve with diamonds*), both in the presence of 2 μM MeAsp, are shown for the case where K_i increases with temperature. The background conditions for the two response curves are labeled by the solid square and diamond in *a*.

In addition to affecting thermotaxis through shifting receptor methylation level, chemical background can also directly interfere with thermosensing if the ligand/receptor binding affinity depends on temperature. In particular, an increase (decrease) of the ligand/receptor dissociation constant $K_{i,a}$ with temperature can induce chemotaxis response toward lower (higher) temperature region where the normalized attractant concentration $[L]/K_{i(a)}$ for constant (but nonzero) ligand background is higher. As a result, the temperature dependence in ligand binding affinity can reduce (increase) the inversion temperature if $K_{i,a}$ increases (decreases) with temperature. This additional change in T_c is verified by our numerical simulation as shown in Fig. 4 *a*, where two critical lines $T_c([L])$ separating the warm sensing regime from the cold sensing regime are plotted for the cases with (Fig. 4, *solid line*) and without (Fig. 4, *dotted line*) temperature dependence of $K_{i,a}$. Two typical cases of temperature impulse responses in the warm and the cold sensing regime are shown in Fig. 4 *b*. The signal integration of both ligand concentration and temperature changes ($T \rightarrow T + \Delta T, [L] \rightarrow [L] + \Delta[L]$) can also be studied in our model (see Supporting Material and Fig. S2 for details).

SUMMARY AND DISCUSSION

In this study, we have developed a quantitative model for *E. coli* thermotaxis by introducing temperature effects in the chemotaxis pathway. By analyzing our model in comparison with existing experiments, a general mechanism for precision sensing in thermotaxis emerges. Although thermotaxis and chemotaxis share the same signaling pathway, their adaptation processes differ significantly, allowing the system to carry out both precision sensing (of temperature) and gradient sensing (of ligand concentration) as illustrated in Fig. 5. Two key differences in the energetic and the kinetic aspects of the adaptation process are identified. First, for gradient sensing, an increase in stimulus strength (ligand concentration) simply shifts the activation free energy $f_t(m,[L])$ as shown in Fig. 5 *a*. Therefore, an increase of attractant concentration always results in a decrease in activity, regardless of receptor methylation level. However, for precision sensing, the external stimulus (temperature) can change (tilt) the dependence of methylation free energy on receptor methylation level m such that $f_t(m,T)$ at different temperatures can cross at a critical methylation level m_c (Fig. 5 *b*). Consequently, the response to a temperature increase is reversed as m increases pass m_c. Second, for chemotaxis (gradient sensing), adaptation kinetics has no (or weak) direct dependence on the signal strength. Therefore, the adapted states (Fig. 5 *a*, *solid circles*) have nearly the same activity, i.e., perfect adaptation to ligand. For thermotaxis (precision sensing), temperature directly affects the adaptation kinetics. Consequently, the activities of the adapted states (solid circles in Fig. 5 *b*) depend on temperature, i.e., imperfect adaptation to temperature. This temperature-

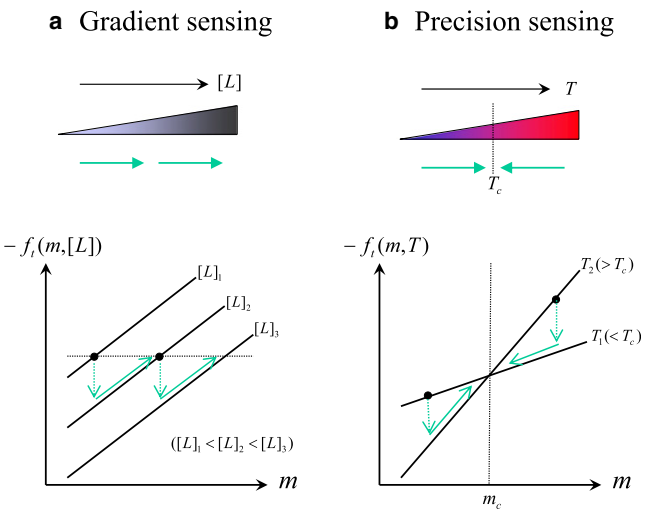

FIGURE 5 The comparison between gradient-sensing and precision-sensing mechanisms. (*a*) For gradient sensing in chemotaxis, increases in ligand concentration simply shift the free energy for kinase activity and result in decreases (*dotted arrows*) of activity for all methylation levels. The adapted states (*solid circle*) have roughly the same activity (perfect adaptation). Decrease in activity (*dotted arrows*) and the subsequent adaptation (*solid arrows*) always lead the system to higher attractant concentrations, i.e., gradient sensing. (*b*) For precision sensing in thermotaxis, temperature change can tilt the kinase activity free energies and $f_t(m,T)$ because different temperatures can cross at a critical methylation level m_c, making receptors warm sensor for $m < m_c$ or cold sensor for $m > m_c$. The adapted states (*solid circles*) have kinase activities that increase with temperature. This temperature-dependent imperfect adaptation kinetics keeps receptors as warm sensors at temperature $T < T_c$ and drives them to become cold sensors at higher temperature $T > T_c$. The activity decreases (*dotted arrows*) and the subsequent adaptation processes (*solid arrows*) drive the system toward $T = T_c$, i. e., precision sensing.

dependent adaptation kinetics is necessary for precision sensing as it drives the receptors to high methylation level $m > m_c$ at $T > T_c$ so that the cell becomes cold sensing at high temperature. In general, T can represent other global factors, whereas m describes the corresponding adaptational state of the system (not limited to single-cell organisms). The mechanism for precision sensing of this global factor should apply provided the two conditions identified in this study are met.

Like Tar receptors, the other major *E. coli* chemoreceptor Tsr is sensitive to temperature (1), albeit with a different methylation level dependence. Tsr changes from warm sensor at low methylation levels to being insensitive to temperature changes at high methylation levels. This temperature-dependent behavior of the Tsr receptor can be captured in our model by modifying the methylation temperature coupling coefficient α_2 in the receptor activation free energy for Tsr. For example, we have used a decreasing but positive function of the Tsr methylation level m_2 for α_2: $\alpha_2(m_2) = m_a e^{-m_2/m_c}$ with constants m_a and m_c. The modified model with mixed receptors (11) can then be used to study thermotaxis in combined chemical environments in the presence of both MeAsp and serine. Because of the different thermosensing characteristics of Tar and Tsr, the behaviors of wild-type cells are

determined not only by the background attractants, but also by the relative abundance of the two types of major chemoreceptors. Our preliminary modeling results show that under the same ligand concentration background, increasing ratio of the two receptors (Tar/Tsr) in the mixed receptor functional cluster can change the cell from warm sensing to cold sensing, consistent with the experiments by Salman and Libchaber (8). The critical temperature is predicted to decease as Tar/Tsr ratio increases. Further detailed comparison between our model and experimental results for various mutant and wt cells with different Tar/Tsr ratio in different attractant backgrounds will shed light on signal integration in the chemotaxis pathway.

Temperature effects are difficult to study because of its ubiquity. Because there is no known feedback from the motor to the chemotaxis signaling pathway (22), we have focused on temperature effects in the receptor free energy and its methylation kinetics to study the dynamics of the receptor kinase activity in response to temperature changes. However, the downstream reactions and the motor response may also depend on temperature. Some of these temperature effects have to be compensatory for the whole system to function properly. For example, the imperfect adaptation at the kinase activity level, which we find to be crucial to explain the inversed temperature response, needs to be compensated at the motor switch to bring the CheY-P level to the narrow response region of the flagella motor switch (23). As shown in Eq. 6, CheY-P level increases with temperature, however, the CheY-P concentration $K_{1/2}$ for the half maximum flagellar motor response also increases with temperature as observed by Turner et al. (24). The temperature dependence of the motor bias is at least less sensitive than that of the CheY-P level, and can even be nonmonotonic depending on the details of various temperature dependent factors, such as the CheY-P level, $K_{1/2}$, and possibly the steepness of the motor response curve (the Hill coefficient). Quantitatively, motor response (to CheY-P level) measurements at the single cell level for different temperatures are needed to make predictions on the motor response in thermotaxis. Indeed, it would be interesting to understand how the temperature dependence of the different components in the whole pathway coordinates to guarantee the robustness of chemotaxis behavior at different temperatures.

Thermotaxis represents a generally desirable function for organisms to search for their preferred environment, i.e., precision sensing. Another well-known example is thermotaxis in *C. elegans* (25–27), where the worm moves toward a preferred temperature set by the temperature at which it was cultured. In *E. coli* thermotaxis, the search for the preferred temperature is carried out by the same gradient-sensing apparatus used in chemotaxis. The preferred temperature is encoded in the adaptation part of the pathway, such as the concentrations and kinetic rates of the adaptation enzymes (CheR, CheB). In addition, because of the difference in thermosensing abilities for Tar and Tsr, the preferred temperature is also a function of the Tar/Tsr ratio in *E. coli*. The *E. coli* Tar/Tsr ratio has recently been found to depend on how cells are grown; in particular, those harvested at a later stage of the log-phase (large optical density) seem to have a larger Tar/Tsr ratio (8). Therefore, the preferred temperature in *E. coli* is also a function of the growth condition. The similarity between the thermotaxis behaviors and the dependence of the preferred temperature on growth condition suggests that there may also be similarity in the underlying mechanism for thermotaxis in these two organisms. It would be interesting to investigate if the way *E. coli* encodes and searches for its preferred temperature is a common mechanism for precision sensing in different biological systems.

SUPPORTING MATERIAL

Ten equations and two figures are available at http://www.biophysj.org/biophysj/supplemental/S0006-3495(09)00892-3.

We acknowledge insightful discussions with Drs. Hanna Salman, Albert Libchaber, and Victor Sourjik on various aspects of thermotaxis. We also thank Dr. Tom Shimizu for sharing unpublished data with us.

This work is partially supported by the National Institute of General Medical Sciences (grant 1R01GM081747-01 to Y.T.), the Chinese Natural Science Foundation (grants 10721403, 10634010 to Q.O.), the Ministry of Science and Technology of China (grant 2009CB918500 to Q.O. and Y.T.), and the China Scholarship Council (fellowship 2008100656 to L.J.).

REFERENCES

1. Maeda, K., and Y. Imae. 1979. Thermosensory transduction in *Escherichia coli*: inhibition of the thermoresponse by L-Serine. *Proc. Natl. Acad. Sci. USA*. 76:91–95.
2. Mizuno, T., and Y. Imae. 1984. Conditional inversion of the thermoresponse in *Escherichia coli*. *J. Bacteriol*. 159:360–367.
3. Sourjik, V. 2004. Receptor clustering and signal processing in *E. coli* chemotaxis. *Trends Microbiol*. 12:569–576.
4. Baker, M. D., P. M. Wolanin, and J. B. Stock. 2006. Signal transduction in bacterial chemotaxis. *Bioessays*. 28:9–22.
5. Hazelbauer, G. L., J. J. Falke, and J. S. Parkinson. 2008. Bacterial chemoreceptors: high-performance signaling in networked arrays. *Trends Biochem. Sci*. 33:9–19.
6. Nishiyama, S.-I., T. Umemura, T. Nara, M. Homma, and I. Kawagishi. 1999. Conversion of a bacterial warm sensor to a cold sensor by methylation of a single residue in the presence of an attractant. *Mol. Microbiol*. 32:357–365.
7. Maeda, K., Y. Imae, J.-I. Shioi, and F. Oosawa. 1976. Effect of temperature on motility and chemotaxis of *Escherichia coli*. *J. Bacteriol*. 127:1039–1046.
8. Salman, H., and A. Libchaber. 2007. A concentration-dependent switch in the bacteria response to temperature. *Nat. Cell Biol*. 9:1098–1100.
9. Paster, E., and W. S. Ryu. 2008. The thermal impulse response of *Escherichia coli*. *Proc. Natl. Acad. Sci. USA*. 105:5373–5377.
10. Tu, Y., T. S. Shimizu, and H. C. Berg. 2008. Modeling the chemotactic response of *Escherichia coli* to time-varying stimuli. *Proc. Natl. Acad. Sci. USA*. 105:14855–14860.
11. Mello, B. A., and Y. Tu. 2005. An allosteric model for heterogeneous receptor complexes: Understanding bacterial chemotaxis responses to multiple stimuli. *Proc. Natl. Acad. Sci. USA*. 102:17354–17359.
12. Keymer, J. E., R. G. Endres, M. Skoge, Y. Meir, and N. S. Wingreen. 2006. Chemosensing in *Escherichia coli*: two regimes of two-state receptors. *Proc. Natl. Acad. Sci. USA*. 103:1786–1791.

13. Mello, B. A., and Y. Tu. 2007. Effects of adaptation in maintaining high sensitivity over a wide range of backgrounds for *Escherichia coli* chemotaxis. *Biophys. J.* 92:2329–2337.

14. Barkai, N., and S. Leibler. 1997. Robustness in simple biochemical networks. *Nature.* 387:913–917.

15. Mello, B. A., and Y. Tu. 2003. Perfect and near-perfect adaptation in a model of bacterial chemotaxis. *Biophys. J.* 84:2943–2956.

16. Yi, T.-M., Y. Huang, M. I. Simon, and J. Doyle. 2000. Robust perfect adaptation in bacterial chemotaxis through integral feedback control. *Proc. Natl. Acad. Sci. USA.* 97:4649–4653.

17. Emonet, T., and P. Cluzel. 2008. Relationship between cellular response and behavioral variability in bacterial chemotaxis. *Proc. Natl. Acad. Sci. USA.* 105:3304–3309.

18. Nishiyama, S.-I., T. Nara, M. Homma, Y. Imae, and I. Kawagishi. 1997. Thermosensing properties of mutant MeAsp chemoreceptors with methyl-accepting sites replaced singly or multiply by alanine. *J. Bacteriol.* 179:6573–6580.

19. Brown, D. A., and H. C. Berg. 1974. Temporal stimulation of chemotaxis in *Escherichia coli*. *Proc. Natl. Acad. Sci. USA.* 71:1388–1393.

20. Alon, U., M. G. Surette, N. Barkai, and S. Leibler. 1999. Robustness in bacterial chemotaxis. *Nature.* 397:168–171.

21. Hong, C. B., D. R. Fontana, and K. L. Poff. 1983. Thermotaxis of *Dictyosetlium discoideum* amoebae and its possible role in pseudoplasmodial thermotaxis. *Proc. Natl. Acad. Sci. USA.* 80:5646–5649.

22. Shimizu, T. S., N. Delalez, K. Pichler, and H. C. Berg. 2006. Monitoring bacterial chemotaxis by using bioluminescence resonance energy transfer: absence of feedback from the flagella motors. *Proc. Natl. Acad. Sci. USA.* 103:2093–2097.

23. Cluzel, P., M. Surette, and S. Leibler. 2000. An ultrasensitive bacterial motor revealed by monitoring signaling proteins in single cells. *Science.* 287:1652–1655.

24. Turner, L., A. D. T. Samuel, A. S. Stern, and H. C. Berg. 1999. Temperature dependence of switching of the bacterial flagella motor by the protein $CheY^{13DK106YW}$. *Biophys. J.* 77:597–603.

25. Hedgecock, E. M., and R. L. Russell. 1975. Normal and mutant thermotaxis in the nematode *Caenorhabditis elegans*. *Proc. Natl. Acad. Sci. USA.* 72:4061–4065.

26. Kuhara, A., M. Okumura, T. Kimata, Y. Tanizawa, R. Takano, et al. 2008. Temperature sensing by an olfactory neuron in a circuit controlling behavior of *C. elegans*. *Science.* 320:803–807.

27. Clark, D. A., C. V. Gabel, H. Gabel, and A. D. T. Samuel. 2007. Temporal activity patterns in thermosensory neurons of freely moving *Caenorhabditis elegans* encode spatial thermal gradients. *J. Neurosci.* 27:6083–6090.